Asian Journal of Atmospheric Environment
Vol. 10-2, pp. 114-123, June 2016
doi: http://dx.doi.org/10.5572/ajae.2016.10.2.114

ISSN (Online) 2287-1160
ISSN (Print) 1976-6912

Chemically Aged Asian Dust Particles Proven by Traditional Spot Test and the Most Advanced micro-PIXE

Chang-Jin Ma, Susumu Tohno[1] and Gong-Unn Kang[2],*

Department of Environmental Science, Fukuoka Women's University, Fukuoka 813-8529, Japan
[1]Graduate School of Energy Science, Kyoto University, Kyoto 606-8501, Japan
[2]Department of Medical Administration, Wonkwang Health Science University, Iksan 54538, Korea

*Corresponding author. Tel: +82-11-8629-7700, E-mail: gukang@wu.ac.kr

ABSTRACT

A change in chemical compositions of Asian dust (AD) particles can dramatically alter their optical properties, cloud-forming properties, and health effects. The present study was undertaken to evaluate this aging of AD particles by means of two complementary methods (i.e., the traditional spot test and the most advanced micro-PIXE analytical technique) for single particle analysis. Size-classified particles were sampled at the rural peninsula of Korea (Byunsan, 35.37N; 126.27E) during AD event and non-AD period in 2004. Sulfate was principally enriched on the particles in the size range of 7.65-10.85 μm collected during AD event. The average number fraction of coarse particles (>2.05 μm) containing chloride was 16.2% during AD event. Relatively low particles containing nitrate compared to those containing sulfate and chloride were found in AD event. Micro-PIXE elemental maps indicated that a large number of AD particles were internally mixed with man-made zinc. The highest peaks of EC and OC concentrations were appeared at 0.01-0.43 μm particle aerodynamic diameter. High EC concentration in PM_1 was might be caused by the Saemangeum Seawall Project that was being conducted during our field measurement.

Key words: Asian dust, Single particle, Byunsan Peninsula, Long-range transport, Spot test

1. INTRODUCTION

The processes of chemical transformation (generally called aging) of mineral particles have been the objective of Asian dust (AD) study for a long time. During long-range transport from the source region to the receptor areas (e.g., Korean Peninsula, Japanese Island, the Pacific Ocean, and West/North America) AD particles experience the complicate aging processes such as capturing of gases, coagulating of solid particles, reacting with each other, cloud processing, and heterogeneous reactions. These aging processes offer the internal mixing of AD particles with secondary species (e.g., sulphate, nitrate, and hydrochloric acid), sea salts, and biomass burning particles (Ma, 2010; Hwang *et al*., 2008; Clarke *et al*., 2004; Zhang *et al*., 2000).

When AD particles passed through clouds, the liquid phase oxidation of SO_2 could have potentially led to increased sulfate on the surface of AD particles (Wurzler *et al*., 2000). When AD particles coated with soluble sulfate they would efficiently become cloud condensation nuclei (CCN) and modify the amount and acidity of precipitation (Zhao *et al*., 2000). The aging of AD particles can also alter the marine ecosystem and the radiative properties of dust clouds (Zhang and Iwasaka, 2004). In addition, it may lead to adverse health effects in humans.

In order to thoroughly understand these denaturations of AD particles, a detailed knowledge of how man-made pollutants and sea-salt aerosol interact with natural individual AD particles is required. Zhang and Iwasaka (1998) carried out the study on the morphological and chemical composition of individual AD particles using the Scanning Electron Microscopy coupled with Energy Dispersive X-ray (SEM-EDX). Zhang and Iwasaka (1999) also reported the internal mixing state of individual AD particles with sulfate and nitrate using the reagent thin film method. Implication of heterogeneous reactivity between $PbSO_4$ and $CaCO_3$ particles for modification of AD particles during long-range transport was performed by Ishizaka *et al*. (2009). Meanwhile, Ma (2010) interpreted the aging of individual AD particles estimated with 2-D elemental maps drawn by the novel double detector system of micro-PIXE (Particle-induced X-ray emission).

However, only a few collaborative studies on between the quantitative analysis for the trace elements and the chemical mixing state of ionic components in individual AD particles, which is desirable to explain the aging processes of AD particles, were reported (Tohno *et al*.,

2006).

In the present study, in order to clarify the aging of AD particles, both two different dual thin-film methods and the novel double detector system of micro-PIXE were applied to the analysis of the size-resolved individual particles collected at a rural peninsula of Korea.

2. MATERIALS AND METHODS

2. 1 Preparation of Two Different Dual Thin-films

A visual spot test is a traditional manual method for the detecting of ionic components (e.g., sulfate, nitrate, and chloride) on individual particles (Mamane and Pueschel, 1980; Ayers, 1977; Bigg *et al*., 1974). This method has apparently not been widely used for particle analysis probably because of difficulties in preparing films, in controlling reactions, in standardizing of the reaction, and in time consuming of the reading. However, this method is still useful to identify the internal mixing state of individual particles with gaseous and secondary aerosol components.

In this study, in order to identify the nitrate, sulfate, mixture of nitrate/sulfate, chloride, and mixture of chloride/nitrate on individual particles collected on AD event, two different dual thin-films were prepared. The dual thin-films (20 nm thickness) of $BaCl_2$/nitron ($C_{20}H_{16}N_4$) and AgF/nitron were prepared by dual simultaneous vacuum deposition of the reagents onto polycarbonate films. And then, two kinds of dual thin-films ($BaCl_2$/nitron and AgF/nitron) were placed on each stage of the impactor. Details of the preparation of two different dual thin-films can be found in elsewhere (Yamasaki *et al*., 2003).

2. 2 Sampling of Size-resolved Particles

Byunsan peninsula of Korea was selected as the sampling site of size-classified particles (Fig. 1). Because of its closeness to China, this site, marked as an empty star in Fig. 1, is the well suited area to measure AD.

Fig. 2 shows the flows of particle sampling and chemical analysis of individual and bulk particles.

For the sampling of aerosols as a function of their size (8-step classification between 0.01 μm and 11 μm), an Andersen air sampler (Tokyo Dylec Co., AN-200) was operated at the ground based site (35.37N; 126.27 E, 30 meters above the sea), indicated by an empty star in Fig. 1.

Quartz filters were put on all stage of Andersen air sampler. Meanwhile, two different dual thin-films ($BaCl_2$/nitron and AgF/nitron) were arranged on the cutoff diameter of five-size steps, i.e., the stage with 7.65 μm, the stage with 5.07 μm, the stage with 3.45 μm, the stage with 2.05 μm, and the stage with 1.17 μm. In addition, for the purpose of identifying the elemental components in individual particles a polycarbonate filter was put on the stage with cutoff diameter of 3.45 μm.

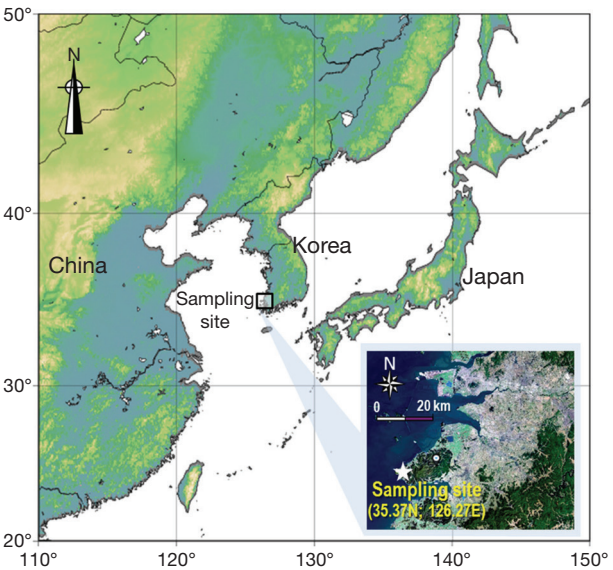

Fig. 1. Maps showing sampling location (an empty star) of Byunsan Peninsula (an empty square).

Our sampling equipment mounting various filter media was intensively operated during AD event (Mar. 30, 2004) and non-AD day (May 26, 2004), respectively. In order to avoid the pile-up of particles, which obscures the chemical determination of particle-to-particle variations, the duration of sampling was adjusted to 20 minutes and 60 minutes at each stage of sampler. After sample collection, every sample was placed in a clean sterilized petridish, they were then sealed with Teflon tape and wrapped with aluminum foil. Every sample was placed in a cold storage bag during air transportation.

On AD and non-AD field campaign days the ranges of wind speed were 2.1-7.8 m s^{-1} and 1.2-4.3 m s^{-1}, respectively and it was generally blowing from the west. The temperatures of AD and non-AD days were around 3.0-12.9°C and 16.7-27.2°C, respectively.

2. 3 Single Particle Analysis Using Micro-PIXE

Fig. 3 shows a schematic diagram of the beam scanning and data acquisition system of micro-PIXE employing double X-ray detectors. The HP-Ge X-ray detector has moderate energy resolution and poor detection efficiency below 2 keV because of its Ge L-shell absorption edge and backscattering proton absorber

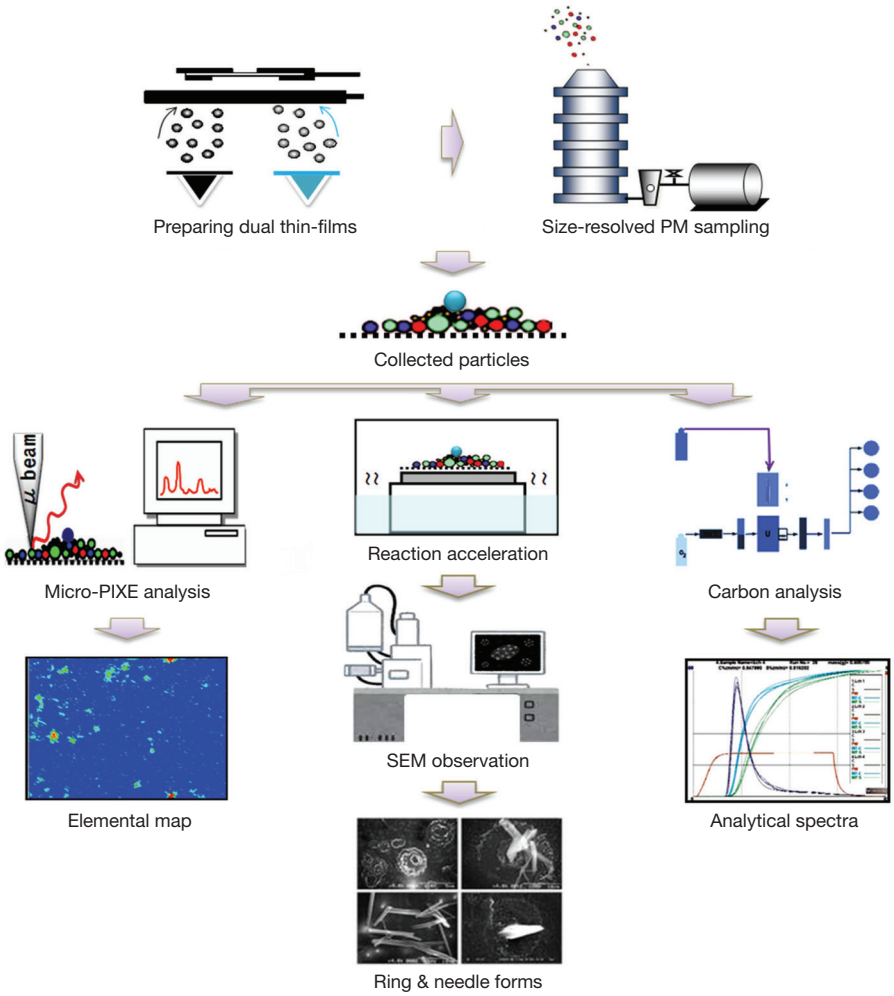

Fig. 2. Flows of sampling and chemical identification of individual and bulk particles.

(60 μm thick polypropylene). The Si(Li) X-ray detector was set at a symmetrical position with the HP-Ge X-ray detector with respect to the beam axis. The energy resolution of the Si(Li) detector is excellent, and this higher energy resolution results in a better signal-to-background ratio and smaller peak overlapping, especially in the low-energy regions. The detector window is 8 μm-thick Be and attached with an annular type absorber (100 μm-thick Mylar) with a center hole (3 mm in diameter). This Si(Li) detector can finally provide a fairly good detection efficiency for X-rays below 2 keV. Details of this double X-ray detectors system for PIXE Analysis have been described elsewhere (Sakai *et al*., 2005).

2. 4 Bulk Analysis for Carbonic Components

The concentration of carbon was determined from the particles deposited on quartz filters using the TOR® (DRI) Method. Two 0.64 cm^2 punches were taken from the quartz filter set on each stage of Andersen sampler and placed in the analyzer. Organic carbon (OC) was defined as all carbon that evolves from the sample without added oxygen when heated up to 550°C. Two additional temperature steps of 700°C and 800°C are made. Elemental carbon (EC) was defined as all carbon that evolves from the sample when heated up to 800°C in 2% oxygen in 98% helium atmosphere after the OC was removed. This TOR® method is a well-accepted technique in which the sample is progressively pyrolyzed with continuous detection of evolved carbon. Chow *et al*. (1993) gave a full detail of TOR® method.

3. RESULTS AND DISCUSSION

3. 1 Air Movement During an AD Event

In order to determine the source region of aerosols at the receptor, i.e., Byunsan peninsula, the atmospheric

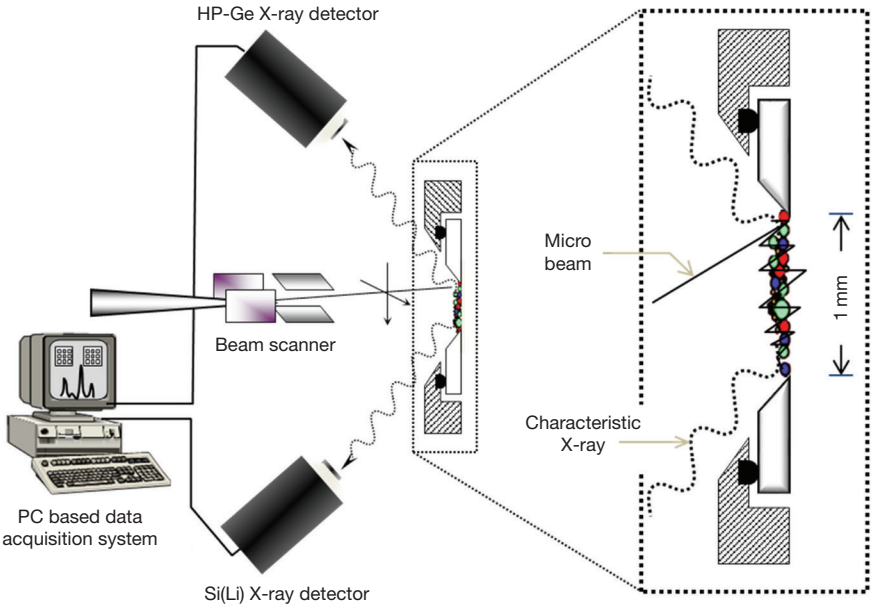

Fig. 3. A schematic diagram of the beam scanning and data acquisition system of micro-PIXE system consisting of the advanced HP-Ge : Si(Li) X-ray detectors.

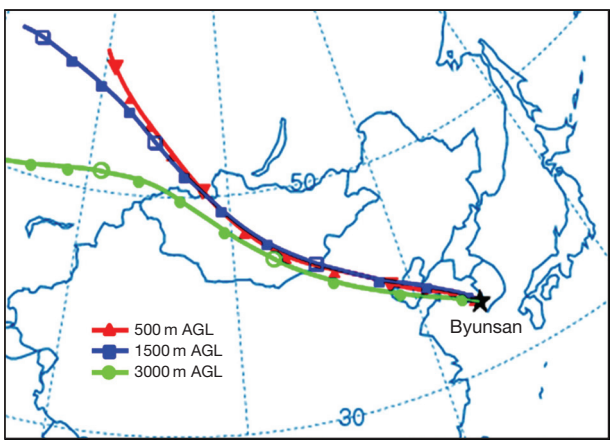

Fig. 4. Backward trajectories at 20 UTC 30 Mar., 2004 drawn by the NOAA HYSPLIT model. Source point (Byunsan) and label interval are 35.37°N; 126.27°E and 6 hours, respectively.

backward dispersion model was applied. Fig. 4 displays the backward aerosol dispersion simulated by the NOAA Air Resources Laboratory (ARL) HYSPLIT dispersion-trajectory model "backwards". A detailed model description of HYSPLIT was given by Rolph (2003).

According to this model results, the air parcels of AD storm on Mar. 30, 2004 was coming from the desert and loess regions in eastern China and southern Mongolia through urban Beijing metropolis by the prevailing winds originated from northwest. And it was extended to the Korean Peninsula after passing through the Yellow Sea.

3. 2 Morphology of Spot Test

In order to promote the reactions between the dual thin-film and the aged ionic components, the dual thin-film loading particles has to be exposed to the adequate solvent vapor atmosphere (Mamane and Pueschel, 1980; Ayers, 1977; Bigg *et al*., 1974).

In the present study, the grids of the dual thin films of $BaCl_2$/nitron and AgF/nitron were exposed to the vapors of ethanol and prophanol/ethanol under room temperature for 24 h. After leaving of thin-films from alcohol environment, the morphologies of spot were photographed by a SEM (HITACHI, S-3000H).

Sulfate and nitrate on and/or in individual particles can be identified by the appearance of the Liesegang ring (i.e., the product of sulfate and barium chloride reaction) and the needle-like bundle (i.e., the product of nitrate and nitron reaction), respectively. Meanwhile, the particles containing chloride and nitrate collected on the dual thin-film of AgF/nitron form AgCl ring and needle crystal, respectively.

Fig. 5 illustrates a $BaSO_4$ ring formed on $BaCl_2$ thin-film, a NO_3 needle crystal formed on nitron thin-film, and the mixture of ring and needle formed on the dual thin-film of $BaCl_2$/nitron. The mixed AgCl ring and needle crystal was also formed on the dual thin-film of AgF/nitron.

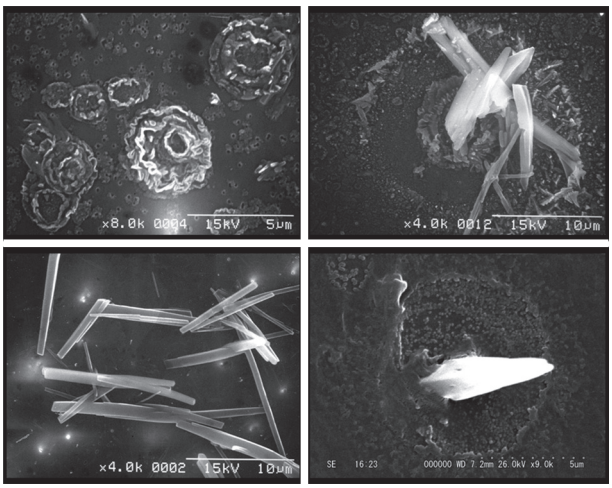

Fig. 5. $BaSO_4$ ring formed on $BaCl_2$ thin film (left upper), NO_3 needle crystal formed on nitron thin film (left down), the mixed ring (sulfate) and needle (nitrate) (right upper) formed on the dual thin film of $BaCl_2$/nitron, and the mixed AgCl ring (chloride) and needle crystal (nitrate) (right down) formed on the dual thin film of AgF/nitron.

3. 3 Morphological Identification of Ionic Components in the Size-classified Individual Particles

Fig. 6 shows the variation of relative number fraction (the number of each ionic species/300 × 100) of each ionic composition and their mixtures identified from the size-classified individual particles collected during AD event. A total of 1,500 individual particles (300 particles from each fraction of 5-step particle size) deposited on the dual thin-films placed on each stage of Andersen sampler was identified. The needle shape crystals formed by nitrate on both the dual thin-films of $BaCl_2$/nitron and AgF/nitron were averaged. The strong particle size-dependent variations were found for the content of ionic compositions and their mixtures. Sulfate showing the maximum number fraction was principally enriched in the particles with big size ($PM_{10.85\text{-}7.65}$). It seems reasonable to say that the enrichment of sulfate in coarse fraction was originated from the heterogeneous mixing with gaseous SO_2 as well as the condensation of H_2SO_4 (or fine sulfate particle) onto dust particles. While on the other hand, a large fraction of sulfate in $PM_{3.45\text{-}2.05}$ was probably due to the cohesion between fine particles which were formed by a gas-to-particle conversion in the atmosphere or the condensation of gases vaporized in the combustion process.

Throughout the one-year observations of size distribution characteristics of major inorganic ions in aerosols at a coastal receptor site in Hong Kong, Bian *et al*. (2014) reported that the dominant presence of sulfate was found in the submicron fraction and its mass fraction in ~0.8 μm was 78-86.9%. They also suggested that nitrate was closely associated with the coarse-mode dust particles as a result of its formation process through the reactions of acidic HNO_3 gas with alkaline components.

Owing to particle sampling considering the limitation of our morphological spot test, unfortunately, a

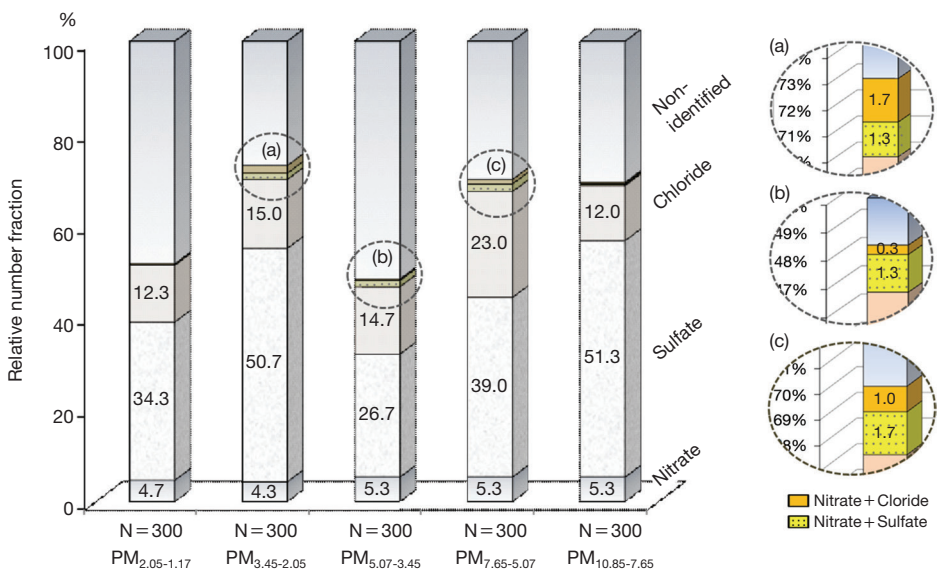

Fig. 6. Relative number fraction of each composition type identified from the size-classified particles collected during AD event at the Byunsan Peninsula by two kinds of dual thin-films. A total of 300 individual particles were identified at each particle size for the two different films.

full explanation of ionic components in the whole size range was not realized in this study.

Through an atmospheric chemistry model study, Xiao *et al*. (1997) reported that the chemical conversion of SO_2 to sulfate on the surface of dust particles might contribute as much as 20-40% of total sulfate in AD particles.

We cannot completely deny the possibility of the presence of mineral $CaSO_4$ contained in coarse mode AD particles. However, even if it existed in the non-aged AD particles, it had almost a negligible impact on our results because the soluble fraction of sulfur is barely existed in the original desert sand of AD (Ma *et al*., 2008).

Ishizaka *et al*. (2009) reported that the major Pb components for the AD particles collected in Japan were PbO, $PbSO_4$, $PbCl_2$, and $PbCO_3$, with molar percentages of 44%, 30%, 21%, and 5%, respectively. This indicates that the Liesegang rings appeared from this $PbSO_4$ contained in AD particles.

The average number fraction of coarse particles (>2.05 μm) containing chloride was 16.2%. This was a little bit higher than that (12.3) of fine particles ($PM_{2.05\text{-}1.17}$). The coarse fraction chloride was probably originated from sea-salts and the mixture of sea-salts and mineral particles. Elsewhere, as a possible source of the coarse fraction chloride, it can be thought that the artificially emitted gaseous Cl into urban atmosphere such as coal-fired power plants, automobiles, and municipal incinerators or the fine particles containing Cl (e.g., NH_4Cl) were absorbed or coalesced with coarse fraction dust particles during long-range transport.

Meanwhile, the nitrate containing particles did not show a strong particle-size depending and they accounted for only 4.3-5.3% through whole particle size. This result was found to be relatively low compared to that of Zhang and Iwasaka (1999). They reported that nitrate was found in some AD particles collected in Beijing, China and the average frequency of nitrate-containing AD particles was 10.8%.

The well-known heterogeneous reactions between gaseous nitrate and coarse particles are below chloride loss and carbonate loss processes.

$$NaCl_{(aq,\,s)} + HNO_{3(g)} \rightarrow NaNO_{3(aq,\,s)} + HCl_{(g)}$$
$$CaCO_{3(s)} + 2HNO_{3(g)} \rightarrow Ca(NO_3)_{2(s)} + H_2O + CO_{2(g)}$$

However, there are many unanswered questions concerning heterogeneous reactions to form aqueous droplets of $Ca(NO_3)_2$ from Ca-rich dust particles under atmospheric conditions, largely owing to a lacking of information on the amount of atmospheric gases and the amount of water vapor needed on particle surface as reactant in the heterogeneous reactions.

The mixtures of nitrate/chloride and nitrate/sulfate showed a very small number fraction (i.e., 0.3-1.7% and 1.3-1.7%, respectively). They have negligible number fractions relative to other ions.

Fig. 7 shows the relative frequency of each composition type identified from the particles collected on a non-AD day. With the exception of nitrate, the frequencies of sulfate and chloride containing particles were much smaller in non-AD period than on AD event. An exceptionally high difference in coarse fraction between two periods suggests that sulfate and chloride were intensely formed on dust particles during their transport from source areas to the Byunsan Peninsula. On the other hand, the frequency of particles involving nitrate increased in a non-AD day in comparison with AD event.

The fossil fuel source dominates the NO_x budget in industrialized areas, while the soil NO emissions control NO_x budgets in remote and rural areas (Delmas *et al*., 1997). From the study of distinguishment between the dominant sources of NO_x emissions: anthropogenic (fossil fuel and biofuel) emission and biomass burning and soil emissions, Sheel *et al*. (2010) suggested that higher temperature leads to more soil emission of NO_x. Therefore, it is also speculated that the high loading of nitrate at Byunsan in the end of May (the maximum temperature on 26 May was 27.2°C) could be due to more local emission of NO_x such as soil emission.

The fact that the internally mixed chloride with nitrate was identified only on AD event is good evidence that the increasing of the number fraction for chloride containing particles on AD event was derived from the aging of dust particles with chloride during long-range transport.

3. 4 Discrimination of the Internally Mixed AD Particles with Hazardous Metallic Component

The aging of AD particles by secondary pollutants is discussed above. Not only these, but many kinds of hazardous metallic components generated from small and large scaled coal combustion facilities including power station contribute to the chemical transformation of AD particles.

Although the standard desert samples of China loess contain an infinitesimal quantity of zinc (59-79 μg g^{-1}) (Sino-Japan Friendship Centre for Environmental Protection), zinc is a good measure of the coal combustion, automobile, and refuse incineration. This has also practical importance in evaluating the health effect of AD particles. The study on the health effects of the metals bound to AD particles conducted by Hong *et al*. (2010) suggested that the exposure of the AD particles containing metals reduces children's pulmonary function.

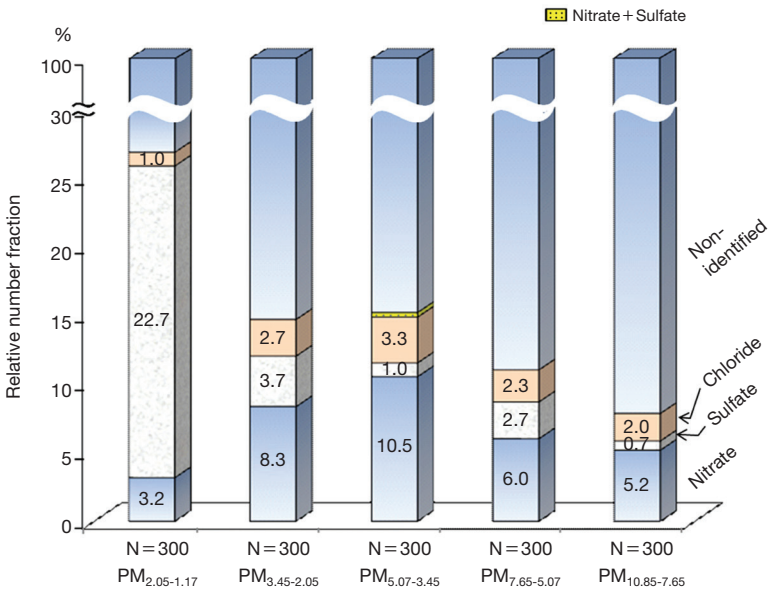

Fig. 7. Relative number fraction of each composition type identified from the size-classified particles collected during non-AD period at the Byunsan Peninsula by two kinds of dual thin-films. A total of 300 individual particles were identified at each particle size.

In this study, an attempt was made to verify the internal mixing of AD particles with zinc based on the visual interpretation of micro-PIXE elemental maps. There are few data regarding the source profile of zinc released to the atmosphere. Although zinc is removed from atmosphere by dry deposition and wet scavenging, however, artificial zinc particles with small sizes and low densities can suspend in the atmosphere and then travel a long distance from emission sources.

Fig. 8 illustrates the elemental maps of silica and zinc and their overlapped elemental mask drawn on and/or in individual coarse ($PM_{5.07-3.45}$) particles collected during AD event. The encircled particles on the overlapped elemental mask indicate the internal mixing of AD particles with zinc. As shown in Fig. 8, a large number of AD particles were internally mixed with zinc.

However, since, as mentioned above, a tiny amount of zinc was detected from the natural and the standard desert samples of China loess, it is necessary to make clear about the sources of the zinc internally mixed with AD particles. To solve this, we investigate correlationships between the micro-PIXE net counts of zinc and those of cobalt. There was a strong correlation between the two with 0.96 R score. Cobalt was not detected from both the natural Asian desert sand (Ma *et al.*, 2008) and the standard desert samples of China loess (Sino-Japan Friendship Centre for Environmental Protection). It could therefore be suggested that zinc contained in numerous particles were originated from artificial sources.

Primary anthropogenic sources of zinc include fossil fuel and waste combustion, and vehicular and aircraft exhausts (Barceloux and Barceloux, 1999). The internal mixture of AD particle with zinc containing particle was probably produced by several mechanisms, such as Brownian coagulation, impaction by differential sedimentation, and coalescence of cloud droplets containing AD particles with those containing zinc particles.

3. 5 EC and OC in Size-resolved PM Collected During an AD Event

Size-resolved concentrations for EC, OC, and TC concentrations are given in Fig. 9. As shown in Fig. 9, a strong bimodal size distribution of EC and OC was found. Both EC and OC concentrations have peaks at 0.01-0.43 μm particle aerodynamic diameter.

Wang *et al.* (2010) measured the size distributions of EC and OC collected in Jiading District, Shanghai. According to their study, the size distributions of both EC and OC showed a bi-modal with peaks in the particles with size of <0.49 μm at one of the most urbanized cities in China. Compared with OC, EC was preferably enriched in this particle fraction. The similar size distribution of carbonaceous compositions was also reported in the former tunnel study (Allen *et al.*, 2001). Allen *et al.* (2001) reported that the aerosol mass concentration mainly composed of EC and OC showed a peak at 0.1-0.2 μm particle aerodynamic diameter collected in the heavy traffic tunnel located in the San Francisco Bay area.

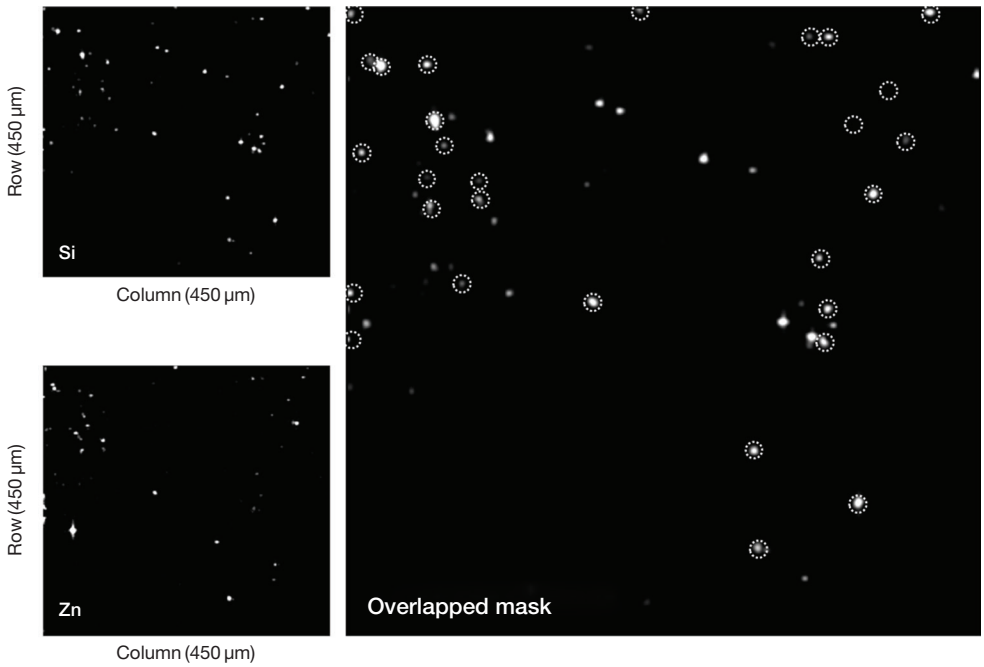

Fig. 8. Elemental maps of silica and zinc (left) on individual coarse fraction ($PM_{5.07\text{-}3.45}$) particles collected during AD event drawn by the micro-PIXE analytical system (scanning area of microbeam: 450×450 μm^2) and their overlapped elemental mask (right).

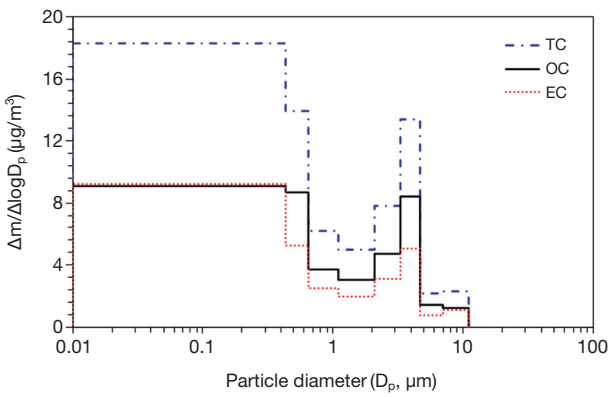

Fig. 9. EC and OC in size-resolved PM collected during AD event.

EC concentration in submicron size fraction of PM measured in this study can be compared to that of measured at Gosan background site in Korea during the Asian Pacific Regional Aerosol Characterization Experiment (ACE-Asia) intensive field campaign. EC concentration in PM_1 in this study was measured as 4.59 μg m^{-3}. Meanwhile, daily mass concentrations of EC at Gosan during non-AD and AD were 0.01-0.9 μg m^{-3} and 0.9-1.6 μg m^{-3}, respectively (Chuang *et al.*, 2003). EC concentration at the Byunsan site of this study was about 4 times higher than that measured at Gosan during AD event. This indicates that the EC concentration of Byunsan site of this study was greatly influenced by other sources. In general, the primary sources of carbonaceous components are vehicle exhaust and industrial emissions. Especially, EC concentration is highest in heavy traffic areas.

One of the reliable causes for high EC concentration at Byunsan site was might be the Saemangeum Seawall Project that was being conducted in our field measurement period. This project completed in April 2006 was the world's longest man-made dike, measuring 33 kilometers and 400 square kilometers of farmland and a freshwater reservoir (Jajuminbo, 2010). It was might be expected that the enormous volume of mobilized equipments including heavy dump trucks and dredging equipments emitted a huge amount of carbon into the local atmosphere.

4. CONCLUSION

Although it is presumed that the chemistry of AD particles can be influenced by absorption of atmospheric gases and subsequent oxidation of the absorbed gases on particle surface during long-range transport, the modification processes of AD particles are still in doubt.

We made an attempt to clarify the aging of AD particles by means of the collaboration between the traditional spot test and the most advanced micro-PIXE analytical technique. The reactions of ionic compounds on particles with the dual thin-films allow us to clearly distinguish sulfate, nitrate, chloride, and their mixtures from the size-resolved individual particles. Although the mechanisms and degrees of aging of AD particle with man-made pollutants differ by case (i.e., the amount of acidic gases and water vapor), with the exception of nitrate that was probably caused by the local sources, much higher frequencies of sulfate and chloride containing particles on AD event than on non-AD day suggest that these were intensely formed on dust particles during their long-range transport. Although the numerical limitation of particles that analyzed and discussed in the present study is apprehensive, a visual spot test applied in this study was useful to evaluate the internal mixing state of individual particles with gaseous and secondary aerosol components. As mentioned previously, owing to both the target of this study (i.e., clarifying the aging of AD particles) and the limitation of our morphological spot test, unfortunately, a through discussion about the ionic and elemental components in the submicron PM was not realized. However, the sufficient amount of information on chemical properties of the whole size-range PM collected in AD events is absolutely necessary to comprehensively understand the complicated aging processes of AD particles in association with their source and emission characteristics.

ACKNOWLEDGEMENT

This paper was supported by Wonkwang Health Science University in 2016. The authors wish to express thanks to Ph.D. A. Morikawa who is an alumna of the Graduate School of Energy Science, Kyoto University for his spot test support. The authors gratefully acknowledge all the members, especially Mr. T. Sakai, in the Advanced Radiation Technology Center, Japan Atomic Energy Research Institute for their help of micro-PIXE analysis. The authors are particularly grateful to Ph.D. R. Cao, Tokyo Dylec Co., for carbon analysis. The authors also express thanks to the NOAA Air Resources Laboratory (ARL) for the provision of the HYSPLIT transport and dispersion model and/or READY website (http://www.arl.noaa.gov/ready.html) used in the present study.

REFERENCES

Allen, J.O., Mayo, P.R., Hughes, L.S., Salmon, L.G., Cass, G.R. (2001) Emissions of size-segregated aerosols from on-road vehicles in the Caldecott tunnel. Environmental Science and Technology 35, 4189-4197.

Ayers, G.P. (1977) An improved thin film sulphate test for submicron particles. Atmospheric Environment 11, 391-395.

Barceloux, D.G., Barceloux, D. (1999) Cobalt. Clinical Toxicology 37, 201-216.

Bian, Q., Huang, X.H.H., Yu1, J.Z. (2014) One-year observations of size distribution characteristics of major aerosol constituents at a coastal receptor site in Hong Kong - Part 1: Inorganic ions and oxalate. Atmospheric Chemistry and Physics 14, 9013-9027.

Bigg, E.K., Ono, A., Williams, J.A. (1974) Chemical tests for individual submicron aerosol particles. Atmospheric Environment 8, 1-13.

Chow, J.C., Watson, J.G., Pritchett, L.C., Pierson, W.R., Frazier, C.A., Purcell, R.G. (1993) The DRI thermal/optical reflectance carbon analysis system: description, evaluation and applications in US air quality studies. Atmospheric Environment 27A, 1185-1201.

Chuang, P.Y., Duvall, R.M., Bae, M.S., Jefferson, A., Schauer, J.J., Yang, H., Yu, J.Z., Kim, J. (2003) Observations of elemental carbon and absorption during ACE-Asia and implications for aerosol radiative properties and climate forcing. Journal of Geophysical Research 108, D23, 8634, doi:10.1029/2002JD003254.

Clarke, A.D., Shinozuka, Y., Kapustin, V.N., Howell, S., Huebert, B., Doherty, S., Anderson, T., Covert, D., Anderson, J., Hua, X., Moore, K.G., McNaughton, C., Carmichael, G., Weber, R. (2004) Size distributions and mixtures of dust and black carbon aerosol in Asian outflow: Physiochemistry and optical properties. Journal of Geophysical Research 109(D15), doi:10.1029/2003JD004378.

Delmas, R., Serça, D., Jambert, C. (1997) Global inventory of NO_x sources. Nutrient Cycling Agroecosystems 48, 51-60.

Hwang, H.J., Kim, H.K., Ro, C.U. (2008) Single-particle characterization of aerosol samples collected before and during an Asian dust storm in Chuncheon, Korea. Atmospheric Environment 42, 8738-8746.

Ishizaka, T., Tohno, S., Ma, C.J., Morikawa, A., Takaoka, M., Nishiyama, F., Yamamoto, K. (2009) Implications of heterogeneous reactivity between $PbSO_4$ and $CaCO_3$ particles for modification of Kosa particles during long-range transport. Atmospheric Environment 43, 2550-2560.

Ma, C.J. (2010) Chemical transformation of individual Asian dust particles estimated by the novel double detector system of micro-PIXE. Asian Journal of Atmospheric Environment 4, 106-114.

Ma, C.J., Kasahara, M., Tohno, S., Kim, K.H. (2008) Physicochemical properties of Asian dust sources. Asian Journal of Atmospheric Environment 2, 26-33.

Mamane, Y., Pueschel, R.F. (1980) A Method for the Detection of Individual Nitrate Particles. Atmospheric Environment 14, 629-639.

Rolph, G.D. (2003) Real-time Environmental Applications and Display system (READY) Website (http://www.arl.noaa.gov/ready/hysplit4.html). NOAA Air Resources Laboratory, Silver Spring, MD.

Saemangeum Development and Investment Agency (2016) About Saemangeum http://www.saemangeum.go.kr/sda/en/sub/why/SMA20001.do

Sakai, T., Oikawa, M., Sato, T. (2005) External scanning proton microprobe - a new method for in-air elemental analysis. Journal of Nuclear and Radiochemical Sciences 6, 69-71.

Sheel, V., Lal, S., Richter, A., Burrowsb, J.P. (2010) Comparison of satellite observed tropospheric NO_2 over India with model simulations. Atmospheric Environment 44, 3314-3321.

Wang, G.H., Wei, N.N., Liu, W., Lin, J., Fan, X.B., Yao, J., Geng, Y.H., Li, Y.L., Li, Y. (2010) Size distributions of organic carbon (OC) and elemental carbon (EC) in Shanghai atmospheric particles. Huan Jing Ke Xue 31, 1993-2001. (in Chinese)

Wurzler, S., Reisin, T.G., Levin, Z. (2000) Modification of mineral dust particles by cloud processing and subsequent effects on drop size distributions. Journal of Geophysical Research 105, 4501-4512.

Xiao, H., Carmichael, G.R., Durchenwald, J. (1997) Long-range transport of SOx and dust in East Asia during the PEM B Experiment. Journal of Geophysical Research 102, 28589-28612.

Yamasaki, S., Onishi, Y., Tohno, S., Kasahara, M. (2003) Development of the multiple thin film method to identify the mixing states of chloride and nitrate ions in individual aerosol particles. Journal of Aerosol Research 18, 34-39 (in Japanese).

Zhang, D., Iwasaka, Y. (1998) Morphology and chemical composition of individual dust particles collected over Wakasa bay, Japan. Journal of Aerosol Science 29, S217-S218.

Zhang, D., Iwasaka, Y. (1999) Nitrate and sulfate in individual Asian dust-storm particles in Beijing, China in spring of 1995 and 1996. Atmospheric Environment 33, 3213-3223.

Zhang, D., Iwasaka, Y. (2004) Size change of Asian dust particles caused by sea salt interaction: Measurements in southwestern Japan. Journal of Geophysical Research 31, L15102, doi:10.1029/2004GL020087.

Zhang, D.Z., Iwasaka, Y., Shi, G.Y., Zang, J.Y., Matsuki, A., Trochkine, D. (2000) Mixture state and size of Asian dust particles collected at southwestern Japan in spring 2000. Journal of Geophysical Research 108(D24), doi: 10.1029/ 2003JD003869.

Zhao, X., Wang, Z., Zhuang, G., Pang, C. (2000) Model study on the transport and mixing of dust aerosols and pollutants during an Asian dust storm in March 2002. Terrestrial Atmospheric and Oceanic Sciences 18(3), 437-457.

(Received 1 April 2016, revised 23 May 2016, accepted 2 June 2016)